Optimal eco-emission scheduling of a microgrid by considering uncertainties

SAEID SHOJAEI[1], JAMAL BEIZA[1,*], TAHER ABEDINZADEH[1], AND HASAN ALIPOUR[1]

[1] Department of Electrical Engineering, Shabestar Branch, Islamic Azad University, Shabestar, Iran
[*] Corresponding author: Jamalbeiza@gmail.com

Manuscript received 09 June, 2021; revised 02 November, 2021; accepted 09 November, 2021. Paper no. JEMT-2106-1306.

This paper describes a scheduling problem formulation to optimize and trade-off economic and emission (Eco-Emission) costs of a microgrid (MG). This MG includes solar parking lots (SPL) and local distributed generation (LDG) with a grid-connected bus to exchange power. The output of this work is an operation instruction that is applicable for the operator of MG. This MG operator (MGO), located in the control center of MG, could select either limited power exchange or unlimited power exchange with the main grid. These conditions are considered as two scenarios for the scheduling problem. The proposed bi-objective eco-emission problem is solved by using the ε-constraint and max-min fuzzy decision-making method. In the last section, the input/output power of MG has been studied taking into account demand response (DR). The simulation of the presented framework is carried out in GAMS software. As investigated the obtained results, exchange power with a main grid has a positive effect in decreasing total emission and economic cost of the MG.

keywords: *Eco-Emission Cost, uncertainties, scenario Tree, scenario reduction, ε-constraint method*

http://dx.doi.org/10.22109/jemt.2021.289829.1306

NOMENCLATURE

Indices

f Index of the linear model of LDG minimum on/off time
i Index of EV
j PL index
k Fuel cell index
l Index of photovoltaic cell
m Energy storage system index
t Sample time index

Parameters

a^j, b^j LDG cost coefficients
${B_{Grid}}^t$ Power transfer price between the MG and upstream net
Cap_j Capacity of plants
$DR^{\max}$ Upper bound of allowable DRP participation
$Dn_{j,f}/Up_{j,f}$ Minimum down/up time limit of LDG
${E_G i}^t$ The emission factor for each unit
${E_{Grid}}^t$ The emission factor of the power purchase from the upper grid
G^t Sunlight irradiation
$load_0^t$ Based load without considering TOU
MUT_j/MDT_j Minimum up/down time of LDG
N_{Ev} Total number of EVs in PL
P_t^{PV} PV power output
$P^j_{LDG,\max}/P^j_{LDG,\min}$ Max/Min power output of LDG
$P_{UG}^{\max}$ Upper bound of injected power of main grid
$P^i_{Ch,\max}$ Upper bound of EV charge amount
$P^i_{Dch,\max}$ Upper bound of EV discharge amount
RD^j, RU^j LDG Ramp up/down rate
$SOC_{\max}/SOC_{\min}$ Max/Min state of charge
$\overline{SOC}$ Max value of predicted SOC value
α Years of the planning horizon
λ The variance of prediction presented EVs in the PL
π_s TPossibility of each scenario
μ TThe average number of presented EVs in the PL

Variables

$C_{LDG}^{j,t}$ The operation cost of LDG
DRP^t Shifted load based on TOU
$load^t$ GEnergy demand considering DRP

$M^{i,t}$ Binary variable for the participation of EV in SPL
$P_{Grid}{}^{t}$ Power transfer between the MG and upstream net
IC_i Investment cost of units
$OC_i^{t,\alpha}$ The operational cost of plants in the planning horizon
$OF1$ The first objective function
$OF2$ The second objective function
P_t^{WT} HThe output power of Wind Turbine
$P_{Ch,Ev}^{i,t}/P_{Dch,Ev}^{i,t}$ EV charging/discharging power
$P_{LDG}^{j,t}$ LDG scheduled power
$SOC^{i,t}$ SOC of EV
$SC_{LDG}^{j,t}$ The startup cost of LDG
SOC_j State of charge of jth EV
$U^{j,t}$ Binary variable for ON/OFF status of LDG

1. INTRODUCTION

Energy hub system (EHS) includes several kinds of generations and storage units to meet several kinds of demands. Combined heat and power (CHP) supplies both heat and power demands. Boilers and heat storage can be utilized to manage thermal loads. Electric vehicles (EVs) are a new kind of loads which increase the peak time of the daily load curve (DLC) [1]. To properly integrate EVs, and have a flat DLC, parking lots (PLs) are located in the power system. Fuel-cell-based EVs are used to reduce the amount of destructive emitted gases produced by vehicles. The combination of the mentioned units is defined as a microgrid (MG). The optimal setting and sizing of MG is the first problem. After installing the proper units, managing them is considered the second problem. First, several studies that are performed on MG planning are investigated to illustrate the main contribution of this study.

In [2], a new active controller was employed to the heating/cooling systems to obtain optimal MG planning results. The effects of the presented controller were investigated in the context of a smart grid with high integration of renewable sources. The optimal performance of a smart MG considering both economic and emission (eco-emission) cost in a short-term study was analyzed by [3]. The authors proposed a stochastic programming model to minimize total eco-emission costs. Authors in [4], proposed an MG with EV parking lots and renewable energies as a case study to investigate its reliability and economic constraints. Enhancing technical issues of a 33-bus distribution network by installing a MG was studied in [5], which was formulated as a bi-objective function. The upper level was defined as a planning problem, and the lower level, which was written as an inner problem, was proposed as economic dispatch to minimize the management and operation costs. Authors in [6] proposed a new approach to solve an optimal configuration of MG. The configuration problem was formulated as a bi-objective function with reliability constraints. Private investor benefits were defined following MGO benefits. The Monte Carlo simulation method (MCSM) was employed to create problem uncertainties. In [7], the uncertain behavior of renewable sources was considered in the economic performance of multicarrier energy systems. In [8], the authors have studied the impact of employing several kinds of demand response programs (DRPs) on the optimal configuration of the CHP system. The objective function was suggested as a cost function, and the DR program with minimum total cost was obtained. The influence of employing DRP on the optimal operation of multi-MG (MMG) was investigated [9]. A hierarchical energy management system (HEMS) was implemented for the optimal operation of MMG by considering the role of the energy management system (EMS). In [10] authors studied the power flow analysis of distributed energy resources (DER). The mentioned work was carried out on a system including solar/wind droop controllers and electronically coupled DERs.In [11] authors proposed a planning problem as an eco-emission. Time of use (TOU)-based DRP was applied to make a flat DLC.In [12], PLs were presented as a virtual power plant, and their effects on the unit commitment problem were investigated. Table 1 summarizes the main contributions and consideration of the literature in this area with a comparison with the proposed model in this study.

Table 1. Comparison of the literature and the proposed model

Reference	DR	Objective functions		Uncertain parameters			Scheduling time horizon	
		Economic	Emission	PV/Wind power	Load	EV	Short-term	Long-term
[13]	✓	✓			✓		✓	
[14]		✓	✓	✓				
[15]		✓	✓				✓	✓
[16]		✓			✓		✓	
[17]		✓	✓				✓	
[18]		✓		✓			✓	
[19]	✓	✓	✓	✓			✓	✓
[20]		✓		✓			✓	
[21]	✓	✓					✓	
Current model	✓	✓	✓	✓	✓	✓	✓	✓

Based on the best of knowledge of the authors and comparisons made in Table1, researchers have not proposed a combined long-term and short-term planning of microgrids considering the uncertainties associated with all the renewable power, load, and EV parameters. Accordingly, this study aimed at filling this research gap by proposing a bi-level economic-emission cost function by using ε-constraint and max-min fuzzy decision method to solve optimal scheduling problem and utilizing the scenario tree approach. To summarize, in this paper, a planning problem is solved with these contributions:

1) Minimizing the total investment cost and the operational cost of MGs considering economic-emission dispatch of the MG units and uncertainties associated with MG parameters.

2) Dealing with uncertainties associated with power output of renewable energy source (i.e., PV system), load of the MG, and charging/discharging behavior of the EV drivers by employing the scenario tree approach.

3) Using ε-constraint and max-min fuzzy decision method to obtain the optimal scheduling problem among the Pareto-optimal solutions with minimum operation cost and emission of pollutant gases

Other sections of this paper are organized as follows: In Section2, the planning problem is formulated considering the objective function and operational constraints of DGs. Section3 depicts the studied MG to evaluate the performance of the proposed model. Section4 investigates the obtained results, and finally, the proposed work is concluded in Section5.

2. PROBLEM DEFINITION

A. Objective function

As mentioned in the previous sections, the planning problem is written as a bi-objective function. The first objective function ($OF1$) includes the total investment cost and the operational cost of the MG. Eq. (??), shows the economic-based cost function.

$$OF_1 = \min f_1(x) = \min \sum_{i=1}^{n} IC_i + \pi_s \times \sum_{t=1}^{24} \sum_{i=1}^{n} OC_i^{t,\alpha} \quad (1)$$

where IC and OC are defined as the total investment and operation costs, respectively. These parameters are introduced as follows:

$$\begin{aligned} & IC = \sum_{j=1}^{N} Cap_j \times Cac_j \\ & OC = \sum_{t=1}^{NT} \sum_{i=1}^{Ng} [u_i^t P_G i^t B_G i^t + Start_{Gi} \times max(u_i^t - u_i^{(t-1)}) + \\ & Shut_{Gi} \times max(u_i^{(t-1)} - u_i^t)] + P_{Grid}{}^t B_{Grid}{}^t] + \\ & \sum_{j=1}^{NPL} OC_j^{PL} \times P_t^{PL} + \sum_{l=1}^{NPV} OC_l^{PV} \times P_t^{PV} + \sum_{k=1}^{NFC} OC_k^{FC} \times P_t^{FC} + \\ & \sum_{m=1}^{NESS} OC_m^{ESS} \times P_t^{ESS} \end{aligned} \quad (2)$$

where $Capj$ and Cac are the capacity of the units and the investment cost of the units The second objective function $(OF2)$ includes an emission cost of the MG. The emission cost is formulated as follows:

$$\begin{aligned} & OF_2 = \min f_2(x) = \min \sum_{t=1}^{NT} Emission\_Cost_t = \frac{n!}{r!(n-r)!} \\ & = \min \sum_{t=1}^{NT} \sum_{i=1}^{Ng} [u_i^t P_G i^t E_G i^t + P_{Grid}{}^t \times E_{Grid}{}^t] \end{aligned} \quad (3)$$

Where, $E_G i^t$ is the emission factor for each unit, and $E_{Grid}{}^t$ is the emission factor of the power purchase from the upper grid.

B. The presented solution approach

In this paper two stage solution method has been proposed to solve bi-objective cost function. As it is illustrated in the Eq. (4), in the first stage by using ε-constraint method, bi-objective function is converted to single objective function. In the second one, by using max-min fuzzy decision method and making a tradeoff between functions, optimal solution is obtained among Pareto optimal front solutions [22].

$$\begin{aligned} & OF = min(Cost^{op}) \\ & s.t \\ & \begin{cases} Em \le \varepsilon \\ allequalityandinequalityconstraints \end{cases} \end{aligned} \quad (4)$$

Max –min fuzzy decision-making approach is described as follows: Step 1: for each Pareto solutions (X_n), define a membership function $\mu^{f_k(X_n)}$ as follows[23]:

$$\mu^{f_k(X_n)} = \begin{cases} 0 & f_k(X_n) > f_k^{\max} \\ \frac{f_k^{\min} - f_k(X_n)}{f_k^{\min} - f_k^{\max}} & f_k^{\min} < f_k(X_n) < f_k^{\max} \\ 1 & f_k(X) < f_k^{\min} \end{cases} \quad (5)$$

Step 2: Maximization of the minimum satisfaction from all objectives as:

$$\max_{N=1}^{N_p}(\min_{k=1}^{N_o}(\mu^{f_k(X_n)})) \quad (6)$$

C. Operational constraints of MG units

All the DGs are modeled by studying uncertainties in this section.

C.1. Modeling the PLs system

The capacity of the EVs' batteries, the state of charge (SOC) level for each EV, the charge/discharge schedule for EVs, and the percentage of EVs in the PL all influence the input and output power of PLs. All these variables are probabilistic in nature. The percentage of EVs on the road is determined by the owner's driving habits [?].This parameter can be given as:

$$EVP_{i,t} = \mu \times (1 + 0.1\lambda) \quad (7)$$

where μ and λ are the random variables that are generated by a normal PDF with the mean value and the standard deviation of 13.7 and 4.5, respectively.The travel distance and battery efficiency determine the initial SOC of batteries. SOC is modeled using a five-step normal distribution. This parameter can be calculated as (8) [25]:

$$SOC_{t,i} = \overline{SOC} \times (1 + \alpha * \delta) \quad (8)$$

where δ is a value of (-2.5,-1.5,0,1.5,2.5) , α and $\overline{SOC}$ are equal to 5% and 0.69, respectively.
For each case, the following values must be determined:

- The realized forecast error in the related scenario is the average value of each interval.
- The probability of each scenario The scenario-based method of initial SOC is demonstrated in1

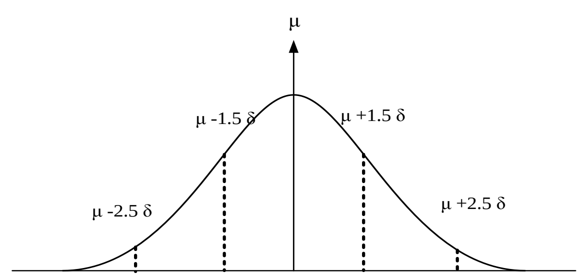

Fig. 1. Five segment probability distribution (PDF) for SOC

The charge/discharge time of EVs are calculated as [25]

$$\begin{aligned} t_{ch} &= \frac{(SOC_{\max} - SOC_j)}{P_v} \\ t_{disch} &= \frac{(SOC_j - SOC_{\min})}{P_v} \end{aligned} \quad (9)$$

The input/output power of EV PL is achieved by considering the introduced parameters as follows:

$$P_t^{PL-in/out} = \sum_{t=1}^{24} \sum_{i=1}^{m} CP_{i,t} \times P_v \times EVP_{i,t} \times SOC_{i,t} \quad (10)$$

D. LDG system modeling

Eq. (11) - Eq. (21) show the constrained model of LDGs. In the first step, operational and startup costs are formulated asEq. (11) - Eq. (13) [?].

$$C_{LDG}^{j,t} = a^j \times U^{j,t} + b^j \times P_{LDG}^{j,t} \quad (11)$$

$$SC_{LDG}^{j,t} \ge \left(U^{j,t} - U^{j,t-1}\right) \times UDC^j \quad (12)$$

$$SC_{LDG}^{j,t} \geq 0 \tag{13}$$

The upper and lower bounds for producing power by LDGs are achieved as Eq. (14), Eq. (15).Rand up and rand down limitations of LDGs are shown inEq. (16), Eq. (17).The minimum up/down times of LDG are limited as Eq. (18), Eq. (19).The minimum up/down of LDGs is shown as a binary form in Eq. (20), Eq. (21) [28].

$$P_{LDG}^{j,t} \leq P_{LDG,\max}^{j} \times U^{j,t} \tag{14}$$

$$P_{LDG}^{j,t} \geq P_{LDG,\min}^{j} \times U^{j,t} \tag{15}$$

$$P_{LDG}^{j,t} - P_{LDG}^{j,t-1} \leq RU^{j} \times U^{j,t} \tag{16}$$

$$P_{LDG}^{j,t-1} - P_{LDG}^{j,t} \leq RD^{j} \times U^{j,t-1} \tag{17}$$

$$U^{j,t} - U^{j,t-1} \leq U^{j,t+Up_{j,f}} \tag{18}$$

$$U^{j,t-1} - U^{j,t} \leq 1 - U^{j,t+Dn_{j,f}} \tag{19}$$

$$\mathrm{Up_{j,f}} = \left\{ \begin{array}{ll} f & f \leq \mathrm{MUT_j} \\ 0 & f > \mathrm{MUT_j} \end{array} \right\} \tag{20}$$

$$\mathrm{Dn_{j,f}} = \left\{ \begin{array}{ll} f & f \leq \mathrm{MDT_j} \\ 0 & f > \mathrm{MDT_j} \end{array} \right\} \tag{21}$$

E. Scenario tree

As mentioned in the last section, demand prediction and output power of the renewable sources and the state of charge/discharge are related to their uncertainties [29]. Figure 2 shows the scenario tree of the planning problem. As illustrated, each scenario starts from the first node (investment cost) and meets the demand in the end node by passing through the leaves. The possibility of each scenario is calculated by multiplying the possibility of the generation and demand uncertainties as well as the possibility of the unit's availability. All the scenarios and states are calculated as follows:$S = \prod_{1}^{75} S_{G,D} \times \prod_{1}^{500} S_A = 30 \times 300 = 9000$. The scenario reduction approach is used to make a trade-off between computational time and accuracy [30]. In this paper, the Kantorovich distance (KD) algorithm is utilized as a probability distance. Eq. (22) shows the approach of KD in reducing problem complexity with scenario reducing [31, 32].

$$[KD(Q,Q') = \inf \left\{ \int\limits_{\varpi \times \varpi'} \begin{array}{l} L(s,s')\eta(ds,ds') \ : \\ \int\limits_{\varpi} \eta(.,ds') = \Omega, \int\limits_{\varpi'} \eta(ds,.) = \varpi' \end{array} \right\} \tag{22}$$

where $L(s,s')$ is a non-negative, continuous, and symmetric cost function, and the infimum is taken over all the joint probability distributions defined in $\varpi \times \varpi'$. $L(s,s')$ that is given as:

$$L(s,s') = \left\|s - s'\right\|^{T} \tag{23}$$

F. . Demand Response program (DRP)

To have an active transferrable load, the DR program is employed as the demand-side management approach. In this paper, all the simulations are carried out by allowing the transferred demand as 20% of the total demand. Eq. (24) - Eq. (27) show how consumers participate in the DR program [33]-[35].

$$Load_t = Load_0 \times (1 - DR^t) \tag{24}$$

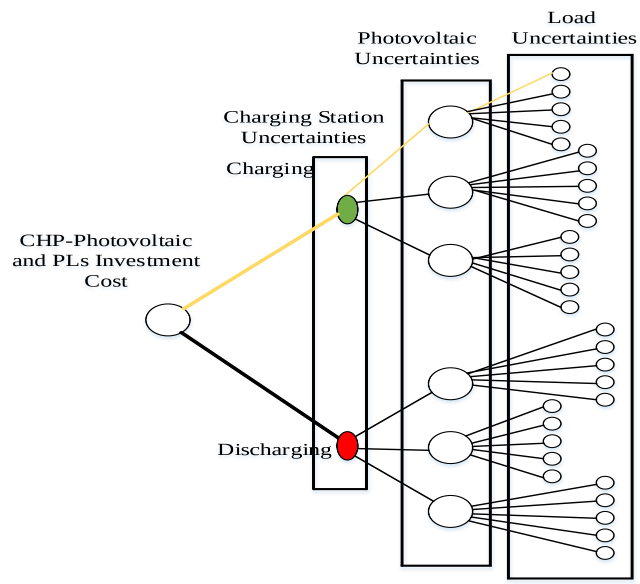

Fig. 2. Scenario tree

$$DR^t \leq DR^{\max} \times Load_0^t \tag{25}$$

$$DR^t \geq -DR^{\max} \times Load_0^t \tag{26}$$

$$\sum_{t=1}^{T} DR^t = 1 \tag{27}$$

3. SIMULATION RESULTS

A. Input data

Fig.3 depicts the proposed MG system. To simulate the planning problem to this system, the input data are given in this section. Two scenarios are studied using the proposed model, including 1: Limited energy exchange with the main grid, and 2: Unlimited energy exchange with the main grid. In both cases, the total electric demand in a day is 1695 kWh, for which the daily load of the MG is shown in Fig.4.The price of purchased energy at each time of the day-ahead market is given in 2. Minimum and maximum operational constraints of LDG are given in 3 3. The cost of power coefficient of DGs is presented in 4 [?]. The amount of generated emission in kg/MWh is given in 5. The maximum output power of DGs is given in 6. Simulation is done using the CPLEX solver of the general algebraic modeling system (GAMS).

B. Numerical investigation

In this section, the obtained numerical results are discussed. As mentioned previously, all the simulations are carried out for two scenarios. The results are given as follows.
A. Scenario 1: Limited energy exchange with the main grid
In this scenario, DGs works in their operational constraints. The required extra energy in the peak demand time has been supplied with the main grid through the grid-connected bus. Table.7 shows optimal obtained results by utilizing the proposed optimization algorithms. The total value of economic and emission costs is $139.7634 and 578.901 kg, respectively.

B. Scenario 2: Un-limited energy exchange with the main grid
In this scenario, the main grid is considered an unlimited unit.

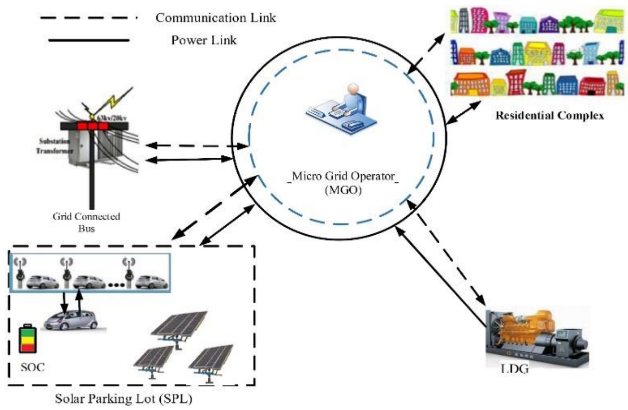

Fig. 3. The Proposed MG configuration

Table 2. Price of Purchased Energy

Time (Hour)	Price ($/kWh)	Time (Hour)	Price ($/kWh)
1	0.23	13	1.5
2	0.19	14	4
3	0.14	15	2
4	0.12	16	1.95
5	0.12	17	0.6
6	0.2	18	0.41
7	0.23	19	0.35
8	0.38	20	0.43
9	1.5	21	1.17
10	4	22	0.54
11	4	23	0.3
12	4	24	0.26

Table 3. Minimum and maximum active power of LDG [37]

Time (Hour)	DG	Maximum Power (kW)	Minimum Power (kW)
1	LDG	30	6
2	Fuel Cell	30	3
3	PV	25	0
4	PL	15	0
5	Battery	30	-30
6	Main Grid	30	-30

Table 4. Coefficients of units operation cost

Time (Hour)	DG	On/Off Cost ($)	
1	LDG	0.96	0.294
2	Fuel Cell	1.65	2.584
3	PV	0	1.073
4	PL	0	0.38
5	Battery	0	0.457

This unit can exchange unlimited power with the proposed MG [37, 38]. As illustrated in Table 8, the value of total cost and the amount of emission are $70.5844 and 528.47 kg, respectively. As can be seen in the numerical results which are tabulated, the optimal efficiency of the proposed algorithm is verified. Furthermore, the obtained results from the simulations revealed that the value of total cost in scenario 2 is reduced compared with scenario 1. MG sells energy to the main grid in the peak load time.

Table 5. Probability of each scenario [4]

Number	DG	NOx	SO2	CO2
		(kg/MWh)	(kg/MWh)	(kg/MWh)
1	LDG	0.1	0.0036	720
2	Fuel cell	0.0075	0.003	460
3	PV	0	0	0
4	PL	0	0	0
5	Battery	0.001	0.0002	10

Table 6. Output active power of DGs

Time (Hour)	PV (kW)/installed (kW)	PL&LDG(MW)
1	0	0.119
2	0	0.119
3	0	0.119
4	0	0.119
5	0	0.119
6	0	0.061
7	0	0.119
8	0.008	0.087
9	0.15	0.119
10	0.301	0.206
11	0.418	0.585
12	0.478	0.694
13	0.956	0.261
14	0.842	0.158
15	0.315	0.119
16	0.169	0.087
17	0.022	0.119
18	0	0.119
19	0	0.0868
20	0	0.119
21	0	0.0867
22	0	0.0867
23	0	0.061
24	0	0.041

4. DISPATCHING POWER OF UNITS

In this section, the dispatching power of each unit in a short time is depicted. Figures 5-8 show the generated electric power of each unit. To properly evaluate the problem, all the figures are illustrated in both conditions, with and without considering the TOU-based DR program. Overall, 20% of the total demand is allowed to participate in the DR program.

The output power of LDGs is illustrated in Fig.5 - Fig.6. As given in the results, according to the operation cost and the amount of emission output of LDG, and considering the price of the main grid, the amount of generated power by LDGs in

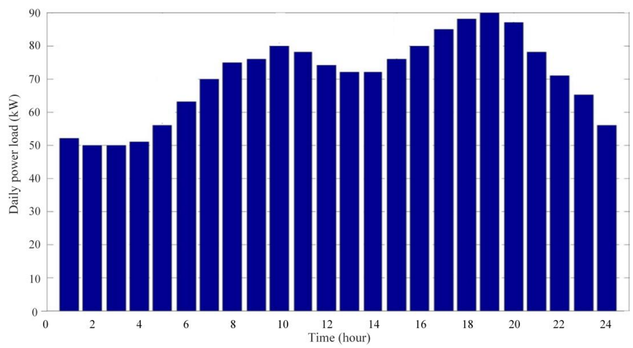

Fig. 4. Daily load of the MG

Table 7. Obtained results of scenario 1

Hour	Main Grid (kW)	Battery (kW)	Parking Lot (kW)	PV (kW)	Fuel Cell (kW)	LDG (kW)
1	30	-14.671	1.7016	0	28.9688	6.0005
2	30	-9.2891	1.8004	0	21.4843	6.0042
3	30	-14.266	1.6443	0	26.3488	6.2728
4	30	-16.778	1.7785	0	29.9995	6
5	30	-8.424	1.8045	0	26.6192	6
6	30	-3.913	0.9143	0	29.9992	6
7	30	8.7861	1.7136	0	23.46	6.04
8	13.7467	23.784	1.3315	0.1376	30	6
9	-19.665	30	1.8198	3.8454	30	30
10	-30	30	12.5372	7.4635	30	30
11	-29.7587	30	8.7213	10.4096	29.9998	28.6296
12	-30	30	10.3649	12.022	30	21.6119
13	-29.9854	30	4.0182	23.705	29.9998	14.2617
14	-30	30	2.4628	20.771	30	18.7661
15	-23.2206	30	1.792	7.4275	30	30
16	-15.4526	30	1.301	4.1512	30	30
17	-7.3746	30	1.8159	0.5584	30	30
18	20.2378	30	1.7622	0	30	6
19	22.5505	29.999	1.5019	0	29.9478	6.0002
20	20.431	30	1.4981	0	29.3587	6
21	-13.778	30	1.2773	0	30	30
22	-18.9564	30	1.3132	0	30	28.6428
23	12.8978	15.192	0.9019	0	30	6.0082
24	30	1.1318	0.521	0	18.3466	6

off-peak time is increased compared with that in on-peak time. Fig.7 shows the remaining SOC of EV in the PL. According to this figure,employing DR encouraged EVs' owners to charge their EV batteries in the off-peak time and discharge and sell it to the grid in the on-peak time. Since sun irradiation is commonly available from 6 A.M to 6 P.M, PV should work at all times without affecting the DR program. Fig.8 demonstrates the output power of the PV unit. Fig.9 shows injected power from the upstream grid in both cases, with and without applying the DR program. As it can be observed, the amount of the purchased power in off-peak time is more than others. Figure 10 shows the effect of applying the DR program in the DLC. As can be seen, by transferring the flexible demands from on-peak time to others, the consumers helped to have a semi-flat DLC. Pareto optimal front in both cases under scheduling short-term study is depicted in Fig.11. Considering this figure, employing the DR improves both emission and economic issues.

Table 8. Obtained results of scenario 2

Hour	Main Grid (kW)	Battery (kW)	Parking Lot (kW)	PV (kW)	Fuel Cell (kW)	LDG (kW)
1	57.9916	-15	0	0	3.0023	6.0609
2	70.9586	-29.2011	0	0	3.0065	6.0021
3	70.9872	-30	0	0	3.0059	6.00689
4	71.9985	-29.999	0	0	3.0005	6
5	76.9909	-30	0.009	0	3.008	6.002
6	72.7249	-18.76	0	0	3.04	6
7	65.1048	-4.1048	0	0	3	6
8	28.1242	10.885	0	0	29.985	6.0004
9	-11.6785	25.884	1.7805	0	30	29.9985
10	-27.9992	25.882	15	7.1205	30	29.9984
11	-31.2727	25.999	8.7723	10.4412	30	29.9985
12	-38.3749	25.999	10.4133	11.9622	30	30
13	-21.9226	30	3.9228	0	30	30
14	-41.4301	30	2.3768	21.049	30	18.7661
15	-15.7802	30	1.7836	0.0001	30	30
16	-11.3521	30	1.3016	0.00256	30	30
17	-4.9875	30	0	0	29.9984	29.958
18	22.0265	29.9818	0	0	29.9982	6.0051
19	24.0215	29.9974	0	0	29.9984	6.0003
20	20.9939	29.9999	0.0032	0	29.3587	30
21	-13.7278	30	1.2773	0	30	30
22	-19	30	0	0	30	6
23	14.0254	15	0	0	29.9852	6.0082
24	46.8957	0.1042	0	0	3	6

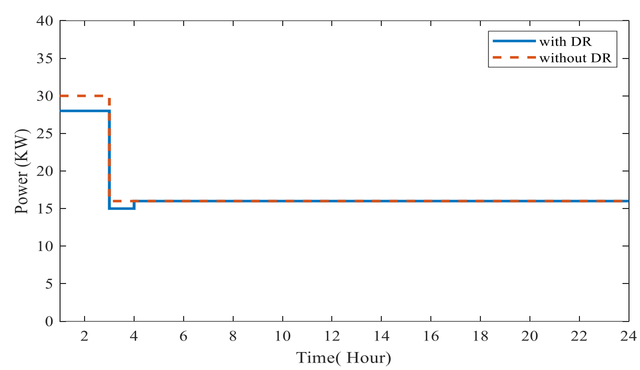

Fig. 5. Output power of LDG1

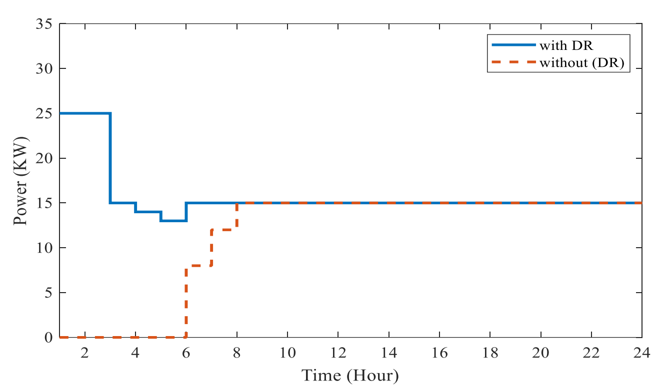

Fig. 6. Output power of LDG2

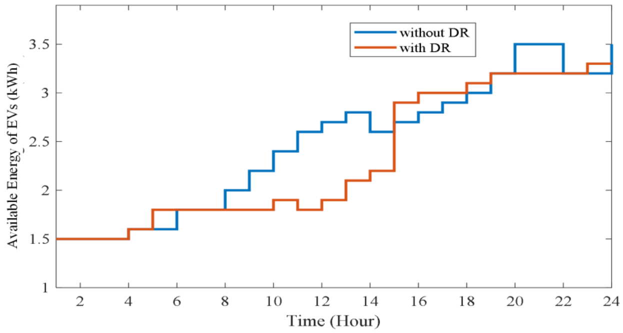

Fig. 7. SOC of EVs in PL

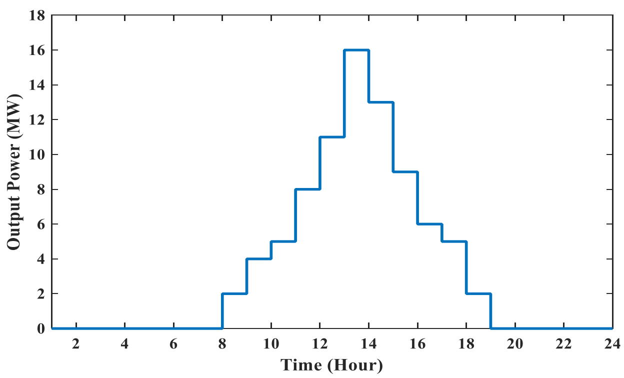

Fig. 8. Output power of PV unit

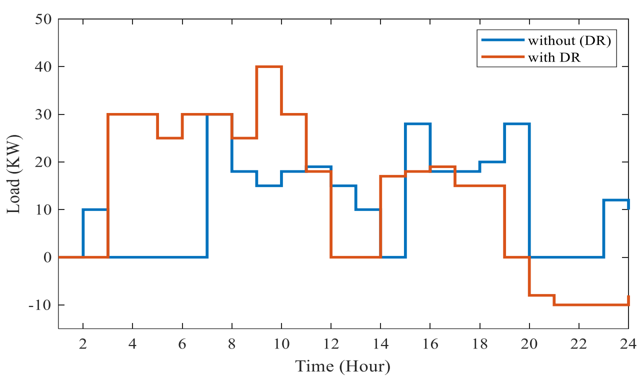

Fig. 9. Injected power from main grid

5. CONCLUSION

The study examined the MG investors' planning decision on minimizing both economic and emission costs. To increase the MG reliability, the planning problem is formulated by considering the grid-connected bus. The amount of power exchange between the grid and MG is evaluated in both conditions, limited and un-limited power exchange. MCS modeled system uncertainties, and the scenario tree is used to illustrate several scenarios and their possibilities. The short-term problem has been written as a bi-objective function, and CPLEX is utilized to minimize total cost. As demonstrated in the results, the obtained results for the total economic and emission cost in case 1 are $139.7634 and 578.901 kg, respectively. These values are changed to $70.56 and 528.48 kg, respectively. Performing a

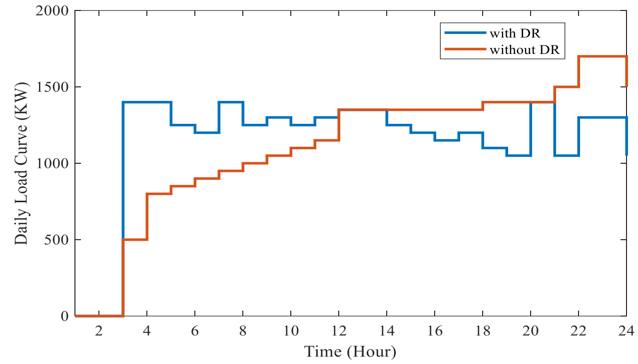

Fig. 10. DLC under employing DR program

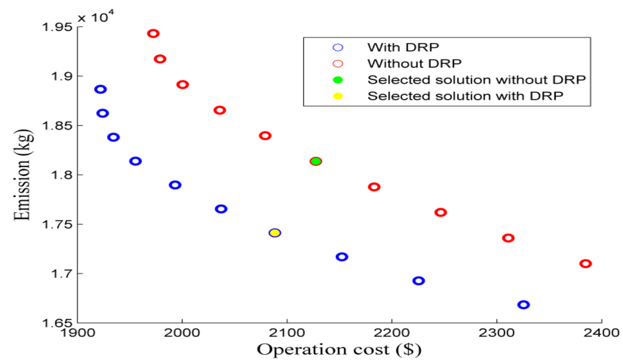

Fig. 11. Optimal Pareto front

comparison, it is observed that the total emission and operation cost of MG under un-limited power exchange with the main grid is decreased up to 49.51 % and 8.06 %, respectively

REFERENCES

1. M. Ghahramani, M. Nazari-Heris, K. Zare, and B. Mohammadi-Ivatloo, "Energy management of electric vehicles parking in a power distribution network using robust optimization method," Journal of Energy Management and Technology, vol. 2, no. 3, pp. 22-30, 2018.
2. J. Chen et al., "Optimal sizing for grid-tied microgrids with consideration of joint optimization of planning and operation," IEEE Transactions on Sustainable Energy, vol. 9, no. 1, pp. 237-248, 2017.
3. F. S. Gazijahani and J. Salehi, "An Efficient Scenario-Based Stochastic Model for Dynamic Operational Scheduling of Community Microgrids with High Penetration Renewables," arXiv preprint arXiv:1711.05614, 2017.
4. A. Awasthi, K. Venkitusamy, S. Padmanaban, R. Selvamuthukumaran, F. Blaabjerg, and A. K. Singh, "Optimal planning of electric vehicle charging station at the distribution system using hybrid optimization algorithm," Energy, vol. 133, pp. 70-78, 2017.
5. S. Mohammadi, S. Soleymani, and B. Mozafari, "Scenario-based stochastic operation management of microgrid including wind, photovoltaic, micro-turbine, fuel cell and energy storage devices," International Journal of Electrical Power & Energy Systems, vol. 54, pp. 525-535, 2014.
6. H. Hosseinnia, D. Nazarpour, and V. Talavat, "Utilising reliability-constrained optimisation approach to model microgrid operator and private investor participation in a planning horizon," IET Generation, Transmission & Distribution, vol. 12, no. 21, pp. 5798-5810, 2018.
7. N. G. Paterakis and M. Gibescu, "A methodology to generate power profiles of electric vehicle parking lots under different operational strategies," Applied energy, vol. 173, pp. 111-123, 2016.

8. H. Hosseinnia, V. Talavat, and D. Nazarpour, "Effect of considering demand response program (DRP) in optimal configuration of combined heat and power (CHP)," International Journal of Ambient Energy, vol. 42, no. 6, pp. 612-617, 2021.
9. A.-D. Nguyen, V.-H. Bui, A. Hussain, D.-H. Nguyen, and H.-M. Kim, "Impact of demand response programs on optimal operation of multi-microgrid system," Energies, vol. 11, no. 6, p. 1452, 2018.
10. H. R. Baghaee, M. Mirsalim, G. B. Gharehpetian, and H. A. Talebi, "Application of RBF neural networks and unscented transformation in probabilistic power-flow of microgrids including correlated wind/PV units and plug-in hybrid electric vehicles," Simulation Modelling Practice and Theory, vol. 72, pp. 51-68, 2017.
11. Hosseinnia, D. Nazarpour, and V. Talavat, "Multi-objective optimization framework for optimal planning of the microgrid (MG) under employing demand response program (DRP)," Journal of Ambient Intelligence and Humanized Computing, vol. 10, no. 7, pp. 2709-2730, 2019.
12. R. A. Waraich, M. D. Galus, C. Dobler, M. Balmer, G. Andersson, and K. W. Axhausen, "Plug-in hybrid electric vehicles and smart grids: Investigations based on a microsimulation," Transportation Research Part C: Emerging Technologies, vol. 28, pp. 74-86, 2013.
13. M. A. Mirzaei, M. Nazari-Heris, B. Mohammadi-Ivatloo, K. Zare, M. Marzband, and S. A. Pourmousavi, "Robust Flexible Unit Commitment in Network-Constrained Multicarrier Energy Systems," IEEE Systems Journal, 2020.
14. H. Karimi and S. Jadid, "Optimal microgrid operation scheduling by a novel hybrid multi-objective and multi-attribute decision-making framework," Energy, vol. 186, p. 115912, 2019.
15. N. E. Koltsaklis, M. Giannakakis, and M. C. Georgiadis, "Optimal energy planning and scheduling of microgrids," Chemical Engineering Research and Design, vol. 131, pp. 318-332, 2018.
16. M. Nazari-Heris, B. Mohammadi-Ivatloo, and S. Asadi, "Optimal operation of multi-carrier energy networks considering uncertain parameters and thermal energy storage," Sustainability, vol. 12, no. 12, p. 5158, 2020.
17. J. Sachs and O. Sawodny, "Multi-objective three stage design optimization for island microgrids," Applied Energy, vol. 165, pp. 789-800, 2016.
18. S. A. Konstantinopoulos, A. G. Anastasiadis, G. A. Vokas, G. P. Kondylis, and A. Polyzakis, "Optimal management of hydrogen storage in stochastic smart microgrid operation," International Journal of Hydrogen Energy, vol. 43, no. 1, pp. 490-499, 2018.
19. M. Quashie, F. Bouffard, C. Marnay, R. Jassim, and G. Joós, "On bilevel planning of advanced microgrids," International Journal of Electrical Power & Energy Systems, vol. 96, pp. 422-431, 2018.
20. M.-N. Heris et al., "Evaluation of hydrogen storage technology in risk-constrained stochastic scheduling of multi-carrier energy systems considering power, gas and heating network constraints," International Journal of Hydrogen Energy, vol. 45, no. 55, pp. 30129-30141, 2020.
21. M. Ghahramani, M. Nazari-Heris, K. Zare, and B. Mohammadi-ivatloo, "Robust short-term scheduling of smart distribution systems considering renewable sources and demand response programs," in Robust Optimal Planning and Operation of Electrical Energy Systems: Springer, 2019, pp. 253-270.
22. A. N. Ghalelou, A. P. Fakhri, S. Nojavan, M. Majidi, and H. Hatami, "A stochastic self-scheduling program for compressed air energy storage (CAES) of renewable energy sources (RESs) based on a demand response mechanism," Energy conversion and management, vol. 120, pp. 388-396, 2016.
23. M. Vahid-Pakdel, S. Nojavan, B. Mohammadi-Ivatloo, and K. Zare, "Stochastic optimization of energy hub operation with consideration of thermal energy market and demand response," energy Conversion and Management, vol. 145, pp. 117-128, 2017.
24. M. J. Mirzaei, A. Kazemi, and O. Homaee, "A probabilistic approach to determine optimal capacity and location of electric vehicles parking lots in distribution networks," IEEE Transactions on industrial informatics, vol. 12, no. 5, pp. 1963-1972, 2015.
25. L. Zhang and Y. Li, "A game-theoretic approach to optimal scheduling of parking-lot electric vehicle charging," IEEE Transactions on Vehicular Technology, vol. 65, no. 6, pp. 4068-4078, 2015.
26. Y. Li et al., "Optimal operation of multimicrogrids via cooperative energy and reserve scheduling," IEEE Transactions on Industrial Informatics, vol. 14, no. 8, pp. 3459-3468, 2018.
27. LI, R., CHEN, L., YUAN, T. et al. "Optimal dispatch of zero-carbon-emission micro Energy Internet integrated with non-supplementary fired compressed air energy storage system," J. Mod. Power Syst. Clean Energy, vol. 4, pp. 566–580 2016.
28. M. Casisi, A. De Nardi, P. Pinamonti, and M. Reini, "Effect of different economic support policies on the optimal synthesis and operation of a distributed energy supply system with renewable energy sources for an industrial area," Energy Conversion and Management, vol. 95, pp. 131-139, 2015.
29. M. Nazari-Heris, S. Abapour, and B. Mohammadi-Ivatloo, "Optimal economic dispatch of FC-CHP based heat and power micro-grids," Applied Thermal Engineering, vol. 114, pp. 756-769, 2017.
30. M. Kia, M. S. Nazar, M. S. Sepasian, A. Heidari, and P. Siano, "An efficient linear model for optimal day ahead scheduling of CHP units in active distribution networks considering load commitment programs," Energy, vol. 139, pp. 798-817, 2017.
31. V. Gholamrezaie, M. G. Dozein, H. Monsef, and B. Wu, "An optimal frequency control method through a dynamic load frequency control (LFC) model incorporating wind farm," IEEE Systems Journal, vol. 12, no. 1, pp. 392-401, 2017.
32. M. Bornapour, R.-A. Hooshmand, A. Khodabakhshian, and M. Parastegari, "Optimal stochastic coordinated scheduling of proton exchange membrane fuel cell-combined heat and power, wind and photovoltaic units in micro grids considering hydrogen storage," Applied energy, vol. 202, pp. 308-322, 2017.
33. N. Nikmehr, S. Najafi-Ravadanegh, and A. Khodaei, "Probabilistic optimal scheduling of networked microgrids considering time-based demand response programs under uncertainty," Applied energy, vol. 198, pp. 267-279, 2017.
34. M. M. Morato, P. R. da Costa Mendes, J. E. Normey-Rico, and C. Bordons, "Optimal operation of hybrid power systems including renewable sources in the sugar cane industry," IET Renewable Power Generation, vol. 11, no. 8, pp. 1237-1245, 2017.
35. Y. Zhang, A. Lundblad, P. E. Campana, F. Benavente, and J. Yan, "Battery sizing and rule-based operation of grid-connected photovoltaic-battery system: A case study in Sweden," Energy conversion and management, vol. 133, pp. 249-263, 2017.
36. V. S. Pappala, I. Erlich, K. Rohrig, and J. Dobschinski, "A stochastic model for the optimal operation of a wind-thermal power system," IEEE Transactions on Power Systems, vol. 24, no. 2, pp. 940-950, 2009.
37. C. Chen, S. Duan, T. Cai, B. Liu, and G. Hu, "Optimal allocation and economic analysis of energy storage system in microgrids," IEEE Transactions on Power Electronics, vol. 26, no. 10, pp. 2762-2773, 2011.
38. H. Moradi, M. Esfahanian, A. Abtahi, and A. Zilouchian, "Optimization and energy management of a standalone hybrid microgrid in the presence of battery storage system," Energy, vol. 147, pp. 226-238, 2018.